Formation of Sweet-Parker-like electron dissipation region in a driven open system

Bin Li[1)], Ritoku Horiuchi[1,2)] and Hiroaki Ohtani[1,2)]

[1)]*The Graduate University for Advanced Studies,322-6 Oroshi-cho, Toki 509-5292, Japan*
[2)]*National Institute for Fusion Science,322-6 Oroshi-cho, Toki 509-5292, Japan*

October 4, 2007

Nonlinear development of collisionless driven reconnection is investigated by making use of the electromagnetic particle simulation code "PASMO" developed for an open system which is subject to an external driving source. The electric field at the reconnection point increases and approaches the external driving field as time goes on. After the formation of x-shaped field structure around the reconnection point, the length of the electron dissipation region continues to increase for a short time. Finally, it stops to grow and relaxes to a steady state when the ratio of the width to length is a constant. Thus, Sweet-Parker-like electron dissipation region is formed in a steady state, while the reconnection rate is controlled by the driving electric field.

Keywords: driven reconnection, collisionless, Sweet-Parker-like, steady state, electrons dissipation region

1 Introduction

Magnetic reconnection occurs in a wide variety of plasma systems, such as collision-dominated plasmas in the solar convection zone, weakly collisional plasmas in the solar corona, and collisionless plasmas in the Earth's magnetosphere, plasma experiments such as tokamak and reversed field pinch[1, 2]. During magnetic reconnection, most of magnetic energy is effectively transformed into plasma energy.

The structure of dissipation region, where reversed magnetic field lines are dissipated and reconnected, has not been understood well for a long time. Recently experimental results [3] of Magnetic Reconnection Experiment (MRX) and observations from WIND satellite [4] shed new light on this research direction. Their results have implied that the dissipation region has a Sweet-Parker like spatial geometry: a long and narrow current layer extends along the downstream direction.

Unfortunately, Sweet-Parker model is simply based on classical collisional resistivity assumption and cannot explain time scale of fast energy release in solar flare. Thus, it is necessary to investigate what mechanism is responsible for breaking the frozen-in flux constraint in the dissipation region. In a series of previous two dimensional simulations, dissipation mechanisms are generally thought to be provided by microscale collisionless kinetic effects, i.e., the inertia effect [5, 6] and the thermal effect [7, 8] based on the non-gyrotropic meandering motion. It is implied that the evolution of collisionless reconnection is controlled by the particle kinetic effects in two dimensions.

In this paper, we will pay attention to investigating steady state of fast magnetic reconnection in a driven case based on the three dimensional particle-in-cell (PIC) code "PASMO" [9, 10]. It is found that in our simulation around the X-line, an electron dissipation region is formed and extended to the downstream. In a steady state, it has a rectangular shape current layer, which is a typical prediction of the Sweet-Parker model.

The outline of the paper is as following; first we describe the simulation model, and second introduce the structure of the electron dissipation region and finally discuss the simulation results.

author's e-mail: li.bin@nifs.ac.jp

2 Simulation model

The simulation is carried out by using three dimensional PIC simulation code "PASMO", 2D version of which has been successfully used in previous investigations[7, 11, 12, 13, 14, 15].

Physical quantities at the boundary of z axis is ($z = \pm z_b$) are assumed to be periodic, upstream and downstream boundaries are set at those of y axis ($y = \pm y_\mathrm{b}$) and x axis ($x = \pm x_b$), respectively.

At upstream boundary, plasmas satisfy the frozen-in condition. By adopting an external electric field $E_z(x, t)$ at $y = \pm y_\mathrm{b}$ along z-axis, ions and electrons are driven into the simulation domain at the same drift velocity. The driving electric field is relatively larger within the input window size x_d around $x = 0$ during the Alfvén time $\tau_A = \mathrm{y_b}/\mathrm{V_A}$, where $\mathrm{V_A}$ is the initial average Alfvén velocity. Therefore, plasmas have larger speed within the size of the input window so as to make the convergent plasma flow into the center of simulation domain where magnetic reconnection will occur first. The driving field will approach a uniform profile with a constant value along the upstream boundary. Magnetic fields can change spatially and temporally according as the driving electric field evolves.

At the downstream boundary $x = \pm x_b$, plasmas number density is controlled by both the charge neutrality condition and the condition of the net number flux, which is associated with the fluid velocity in the vicinity of the boundary [14]. Thus, the plasma can freely flow in or out, the total number of particles may vary with time in this open system. The field quantities E_x,E_y and $\partial_x E_z$ are continuous at downstream boundaries. The other components of the electromagnetic field can be obtained by solving the Maxwell equations at the boundary.

One-dimensional Harris sheet equilibrium is adopted as an initial condition, where magnetic field and plasma pressure are given by $B_x(y) = B_0 \tanh(y/y_h)$ and $P(y) = B_0^2/8\pi \cdot sech^2(y/y_h)$ with the scale height y_h. As a consequence of initially reversed magnetic field configuration, a neutral sheet appears at the center of y axis ($y = 0$). The Lorentz force pushes plasmas toward neutral line, while plasma pressure makes plasmas move away from it. Thus the initial equilibrium is maintained by two forces counterbalance. The distribution of particles is a shifted Maxwellian with a uniform temperature $T_{i0} = T_{e0}$. We set the particle mass ratio $m_i/m_e = 100$, the ratio of plasma frequency to the electron cyclotron frequency $\omega_{pe0}/\omega_{ce0} = 2$, the strength of the inflow velocity $E_0/B_0 = -0.04$, and the ratio of input window size to inflow direction length $x_d = 1.5$ in our numerical simulations.

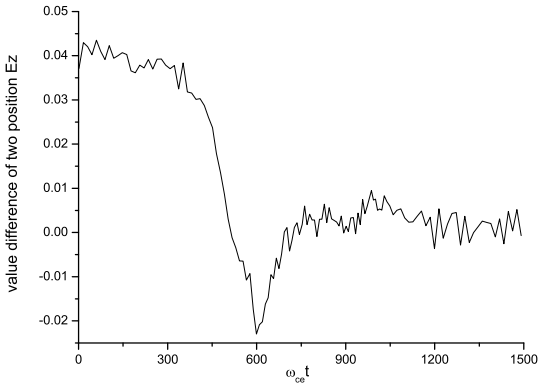

Fig. 1 Difference of electric fields at X-line and upstream boundary as a function of time.

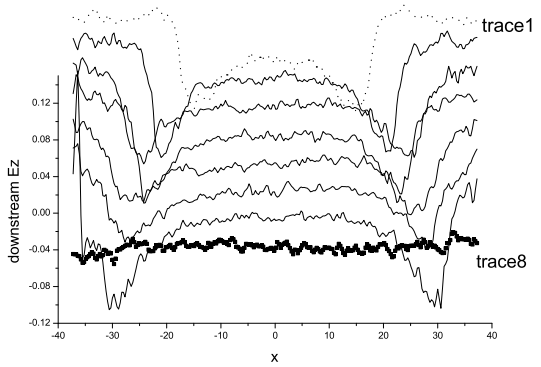

Fig. 2 Spatial profile of electric field E_z along the outflow direction at eight consecutive time periods, where trace 1 denotes the profile at $t\omega_{ce} = 662$, trace 8 at $t\omega_{ce} = 1148$. The reference level of each line is shifted vertically to avoid overlapping of lines.

3 Electron dissipation region

In our simulation model, reconnection rate equals to the electric field at the X-line[7, 9, 10, 11, 12, 13, 14, 15]. When system relaxes to a steady state, both electric field E_z in the system and reconnection rate should equal to the external driving electric filed. After reconnection process begins, the electric field at X-line increases and equals to the driving field after $t\omega_{ce} = 750$. The difference between electric fields at the X-line and upstream boundary is shown in Fig.1. However, the electric field along the downstream direction does not reach uniform profile until $t\omega_{ce} \approx 1110$,as shown in Fig.2. After then, the electric field becomes equal to the driving field everywhere in the system, and thus the system relaxes to the steady state.

Fig.3 shows spatial profile of electrons current density at $t\omega_{ce} = 900$. The electron current density evolves gradually in a long and narrow rectangular region at the center of current layer. Thus, electron current sheet is formed in a narrow and long shape, which is the typical result predicted in the Sweet-Parker model. The current density increases from upstream boundary to the X-line in the inflow direction and magnetic field B_x gradient also increases. To understand the structure of the current sheet, let us consider three spatial scales: electrons meandering motion scale l_{me}, skin depth $d_e = c/\omega_{pe}$, and half width of the sharp peak in the current density profile. The electron meandering scale is defined by the distance which satisfies the condition $\rho_e(y)/y = 1$ [5, 6], where $\rho_e(y)$ is the local electron Larmor radius. The half width of the current density sharp peak is defined by the half width at 80% maximum value of the current density. In Fig.4, time evolution of three spatial scales defined above are plotted, where they are normalized by Debye length and are measured along the vertical line through the X-line. The half width of the sharp peak value is close to the electrons meandering motion scale and has similar tendency in time evolution. This result implies that electrons dynamics control the current sheet formation around the X-line and thus a Sweet-Parker-like electrons dissipation region is generated.

In a kinetic regime non-ideal effects becomes significant through microscopic physical processes and macroscopic frozen-in condition is not satisfied [8, 12, 13, 14, 15]. Ion spatial scale in which non-ideal effects becomes significant for ions are larger than that for electrons. In other words, wider ion dissipation region is formed in the current sheet compared with electron dissipation re-

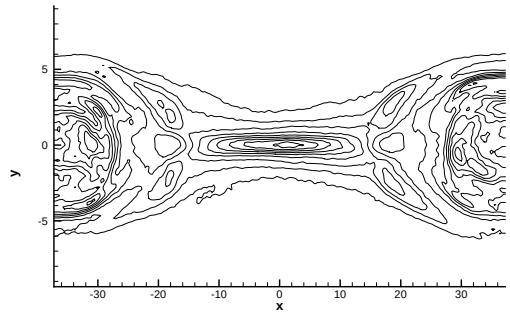

Fig. 3 Spatial profile of electrons current density at $t\omega_{ce} = 900$.

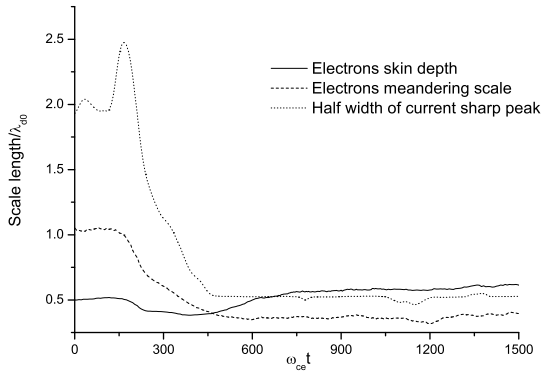

Fig. 4 Time evolution of three spatial scales; electron skin depth, electron meandering scale, and half width of current density peak.

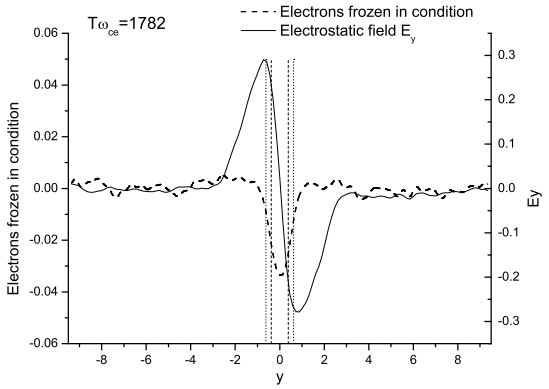

Fig. 5 Spatial profiles of electron frozen-in condition $(E + v_e \times B)_z$ and electrostatic field E_z along the inflow direction. Positions of electron skin depth and meandering scale are indicated by vertical dotted lines and dashed lines, respectively.

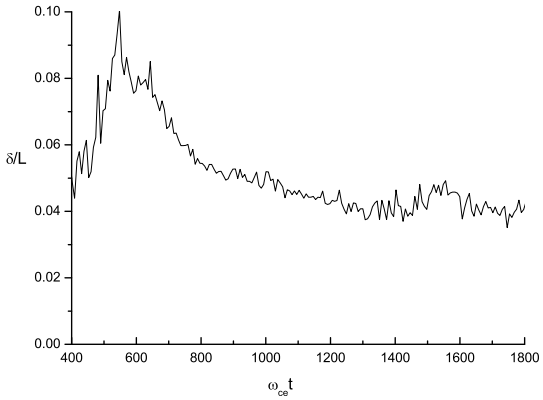

Fig. 6 Time evolution of the ratio of electron dissipation region width to its length.

gion. Figure 5 demonstrates the spatial profiles of electron frozen-in condition $(E + v_e \times B)_z$ and the electric field E_y. Because electrons remains magnetized while ions are not magnetized in the ion dissipation region, the driving field pushes mainly electrons inward and creates electron rich region inside the electron dissipation region. The in-plane electrostatic field is generated due to the charge separation in the kinetic regime and is largest at edge of electrons dissipation region, as shown in Fig. 5. The violation of electron frozen-in condition starts at electrons skin depth and becomes significant below the electron meandering scale

In the steady state, spatial configuration of magnetic field does not change with time and thus the width of electron dissipation region is expected to be a constant too, which is defined by the electrons skin depth. After reconnection rate becomes a constant ($t\omega_{ce} = 750$), the skin depth also becomes constant. Based on the electrons mass conversation let us define the length of the electrons dissipation region by the distance from the X-line to the position where electrons outflow speed is maximum. The ratio of these two scales, $r = d_e/l_e$, can be used to evaluate the structure of electrons dissipation region. In Fig.6, time variation of this ratio is plotted. Although the reconnection rate, electrons skin depth and its meandering motion scale already becomes constant(see in Figs.1 and 4), the curve still gradually decreases after that. The length of electrons dissipation region increases until $t\omega_{ce} \approx 1100$ and then the ratio becomes constant finally. This result corresponds the fact that the electric field in the downstream reaches a constant profile at $t\omega_{ce} \approx 1100$ (see Fig.2).

4 Summary

We have found that a Sweet-Parker-like electron dissipation region is formed during the process of magnetic reconnection. Its width is determined by electron skin depth while its length is defined by the distance from X-line to the position where electron outflow speed has maximum value. The electron dissipation region is mainly controlled by microscopic electron dynamics.

It should be mentioned that there is the delay in the

period when inflow and outflow regions relax to the steady state. The length of electrons dissipation region and downstream electric field E_z still evolve in a while after reconnection rate at the X-line already become equal to diving electric field. The length of electron dissipation region is determined by using the position where electron outflow speed has maximum value. This means that the electron outflow speed starts to decrease as soon as they move into the ion dissipation region, and it gradually approaches the ion outflow speed. The simulation result also indicates that the ratio of the width of the electron dissipation region to its length is approximately given by $\frac{1}{2}(m_e/m_i)^{1/2}$. Thus, the relaxation of electron outflow speed may be determined by the cooperative action of both ion and electron dynamics. The details about this will be discussed in a future paper.

[1] D. Biskamp, *Energy Conversion and Particle Acceleration in the Solar Corona* (Springer Berlin/Heidelberg, Germany, 2003) p.109.

[2] E.Priest and T.Forbes, *Magnetic reconnection* (Cambridge University Press, Cambridge, UK, 2000) p.322.

[3] Hantao Ji, Masaaki Yamada, Scott Hsu, and Russell Kulsrud, Phys. Rev. Lett. **80**, 3256 (1998).

[4] M. Oieroset, T. D. Phan, M. Fujimoto, R. P. Lin and R. P. Lepping, Nature. **412**, 414 (2001).

[5] M. Ottaviani and F. Porcelli, Phys. Rev. Lett. **71**, 3802 (1993).

[6] Biskamp, E. Schwarz, and J. F. Drake, Phys. Rev. Lett. **75**, 3850 (1995).

[7] R.Horiuchi and T.Sato, Phys. Plasmas. **1**, 3587 (1994).

[8] M.Hesse,K.Schindler,J,Bim, and M.Kuznetsova, Phys. Plasmas. **6**, 1781 (1999).

[9] H. Ohtani, R. Horiuchi and A. Ishizawa, J. plasma phys. **72**, 929 (2006).

[10] R. Horiuchi, H. Ohtani and A. Ishizawa, J. plasma phys. **72**, 953 (2006).

[11] R.Horiuchi and T.Sato, Phys. Plasmas. **4**, 277 (1997).

[12] A.Ishizawa, R. Horiuchi, and H. Ohtani, Phys. Plasmas. **11**, 3579 (2004).

[13] W. Pei, R. Horiuchi and T. Sato, Phys. Plasmas. **8**, 3251 (2001).

[14] A. Ishizawa and R. Horiuchi, Phys. Rev. Lett. **95**, 45003 (2005).

[15] W. Pei, R. Horiuchi and T. Sato, Phys. Plasmas. **8**, 3251 (2001).